A simple method to include vertical resolution in a river model, and results from an implementation

Flemming Jakobsen[1], Kim Wium Olesen[2] and Mads Madsen[2]

[1]DHI Water & Environment (M) Sdn. Bhd., 11th Floor, Hill-View Side, Wisma Perindustrian, Jalan Istiadat, Likas, 88400 Kota Kinabalu, Sabah, Malaysia E-mail: *flj@dhi.com.my*

[2]DHI Water & Environment, River and Flood Management Department, Agern Allé 11, DK-2970 Hørsholm, Denmark

Received 13 March 2003; accepted in revised form 3 November 2004

Abstract A simple method to include vertical resolution in a one-dimensional river model is outlined. The equations on which the method is based are the width-averaged continuity, momentum and transport equations. Some details are given on how to formulate the bed friction in a river model with vertical resolution. The equations are transformed to be in sigma coordinates. The numerical techniques, which make maximum use of an already implemented numerical solution technique in an existing river model, are described. The method is used to implement vertical resolution in the existing river model, MIKE 11. The implementation is tested on the following cases: logarithmic velocity profile, wind driven velocity profile, rapid accelerated flow, lock exchange and finally wind-forced entrainment. All test cases showed good agreement.

Keywords Numerical model; river; stratification; vertical resolution

Nordic Hydrology **Vol 36 No 2 pp 163–174** © IWA Publishing 2005

Nomenclature

a_T (K^{-1})	expansion coefficient
A (m^2)	cross-section area
c	concentration, e.g. of temperature, salinity, sediment, etc.
C ($m^{0.5}\,s^{-1}$)	Chezy number
C_{xz} ($m^{0.5}\,s^{-1}$)	Chezy number dependent on level
d (m)	local water depth
D (m)	maximum water depth
g ($m\,s^{-2}$)	gravity
h (m)	interface position
I (−)	surface slope
k (m)	Nikuradse's roughness
p ($N\,m^{-2}$)	pressure
P (m)	wet perimeter
q ($m^3\,s^{-1}\,m^{-1}$)	discharge per width
q_0 ($m^3\,s^{-1}\,m^{-1}$)	lateral inflow
Q_{j-1}^{n+1} ($m^3\,s^{-1}$)	discharge at time step $n+1$ in the $j-1$ grid point
Q_{j+1}^{n+1} ($m^3\,s^{-1}$)	discharge at time step $n+1$ in the $j+1$ grid point
R_f^T (−)	bulk flux Richardson number
S_c	source term
t (s)	time
T (K)	temperature, where index S and B is for surface and bed, respectively
$\underline{u}$ ($m\,s^{-1}$)	velocity in the horizontal x direction

U_f (m s^{-1})	friction velocity
U_t (m s^{-1})	speed of the head
w (m s^{-1})	velocity in the vertical z direction
w_S (m s^{-1})	surface velocity
W (m)	width
x (m)	horizontal coordinate
z (m)	vertical coordinate
z_B (m)	bed level
α_j (−)	coefficient related to the j grid point
β_j (−)	coefficient related to the j grid point
δ_j (−)	coefficient related to the j grid point
Δ (−)	dimensionless reduced density
γ_j (−)	coefficient related to the j grid point
η_j^{n+1} (m)	water level at time step $n+1$ in the j grid point
κ (−)	von Kármán's constant
ν_T (m^2 s^{-1})	turbulent viscosity
ν_{Tx} (m^2 s^{-1})	horizontal turbulent diffusion
ν_{Tz} (m^2 s^{-1})	vertical turbulent diffusion
θ	temporal weighting coefficient between 0 and 1
ρ (kg m^{-3})	water density
ρ_0 (kg m^{-3})	reference density
ρ_S (kg m^{-3})	water density at the surface
σ (−)	sigma coordinate
τ_B (N m^{-2})	bed shear stress
τ_{xz} (N m^{-2})	horizontal shear stress

Introduction

There are many one-dimensional (1D) river models and today they are used both in research and practical engineering consultancy work. A description of the governing equations, etc., on which the models are based, as well as some of the early models, can be found in, for example, Abbott (1979) and Cunge *et al.* (1980). The models sometimes include descriptions of sediment transport/morphology and biological systems. The 1D river models produce useful and trustworthy results in rivers and channels with a homogenous water column, but at locations with stratified conditions they do not always produce trustworthy results. Stratified conditions are, for example, typically found in a reservoir due to the vertical sediment and/or temperature distribution, in a lake due to the vertical temperature distribution and in an estuary due to the vertical salinity distribution. Thus vertical resolution is sometimes needed in the river models in areas where stratified conditions prevail. At the same time, including vertical resolution in non-stratified areas should not change the results significantly compared to the results obtained without vertical resolution.

It is a demanding task to develop an 'easy to use and generally applicable' 1D river model. Not only should the equations be discretized, implemented and tested, and loops and structures be considered, but also graphical user interfaces and GIS are demanded. For that reason it can be highly beneficial if an existing 1D model is at hand and a vertical resolution can be included in this model using the already implemented numerical methods. In the following we will describe such a method.

The method is developed and implemented in MIKE 11, but the method can also be used in other river models. MIKE 11 is based on the finite difference scheme called the Abbott–Ionescu scheme (Abbott and Ionescu 1967), i.e. the computational grid separates water level and discharge. After discretization of the governing equations one ends up with a set of

equations, which should be solved as follows:

$$\alpha_j Q_{j-1}^{n+1} + \beta_j \eta_j^{n+1} + \gamma_j Q_{j+1}^{n+1} = \delta_j \tag{1a}$$

where α_j, β_j, γ_j and δ_j are coefficients related to the j grid point, Q_{j-1}^{n+1} and Q_{j+1}^{n+1} ($\mathrm{m^3\,s^{-1}}$) are discharges at time step $n+1$ in the $j-1$ and $j+1$ grid point, respectively, η_j^{n+1} (m) is the water level at time step $n+1$ in the j grid point and

$$\alpha_j \eta_{j-1}^{n+1} + \beta_j Q_{j,k}^{n+1} + \gamma_j \eta_{j+1}^{n+1} = \delta_j. \tag{1b}$$

Equation (1a) is a derivative approximation to the continuity equation, while Equation (1b) is a derivative approximation to the momentum equation. Thus, the basic idea behind the method outlined later is to rewrite the derivative approximations, which should be solved in the stratified areas, into the same form as Eqs. (1a, b). Let the existing model solve this set of equations and, after the water level and discharges are found, use the original derivative approximations to determine the vertical velocity distribution, etc.

The paper is structured as follows. First, the governing equations are outlined and some details on the bed friction are given. Second, the numerical method is described in detail. Third, the method is implemented in MIKE 11 and the test results are presented. The paper ends with a discussion and a conclusion on the work.

Governing equations

The governing equations consist of the width-integrated continuity, momentum and transport equations. The width-integrated continuity equation is written as

$$\frac{\partial (Wu)}{\partial x} + \frac{\partial (Ww)}{\partial z} = \frac{q_0}{\mathrm{d}z} \tag{2}$$

where W (m) is the width, u and w ($\mathrm{m\,s^{-1}}$) is the velocity in the horizontal (x) and vertical (z) directions, respectively, and q_0 ($\mathrm{m^3\,s^{-1}\,m^{-1}}$) is the lateral inflow (if found needed, the lateral inflow can easily be distributed over depth). The width-integrated momentum equation is written as:

$$W \frac{\mathrm{d}u}{\mathrm{d}t} = -\frac{W}{\rho_0}\frac{\partial p}{\partial x} + \frac{\partial (W \tau_{zx}/\rho_0)}{\partial z} - \frac{\tau_B}{\rho_0}\frac{\mathrm{d}P}{\mathrm{d}z} \tag{3}$$

where t (s) is the time, ρ_0 ($\mathrm{kg\,m^{-3}}$) is the reference density, p ($\mathrm{N\,m^{-2}}$) is the pressure, τ_{xz} ($\mathrm{N\,m^{-2}}$) is the horizontal shear stress, τ_B ($\mathrm{N\,m^{-2}}$) is the bed shear stress and P (m) is the wet perimeter. Finally, the width-integrated transport equation is written as:

$$\frac{\partial Wc}{\partial t} + \frac{\partial Wuc}{\partial x} + \frac{\partial Wwc}{\partial z} = \frac{\partial}{\partial x}\left(W \nu_{Tx} \frac{\partial c}{\partial x}\right) + \frac{\partial}{\partial z}\left(W \nu_{Tz} \frac{\partial c}{\partial z}\right) + WS_c \tag{4}$$

where c is a 'concentration', for example, of temperature, salinity, sediment, etc., ν_{Tx} and ν_{Tz} ($\mathrm{m^2\,s^{-1}}$) is the horizontal and vertical turbulent diffusion, respectively, and S_c is a source term. Even though the transport equation is very important we will not focus on this equation in the following. The methods outlined and used in the continuity and momentum equations are also applicable in the transport equation, and thus it is of no principal interest to also describe the method for the transport equation. It should, however, be noted that the turbulent diffusions are determined by either a constant value, a mixing-length theory, k or a k–ε turbulence model (e.g. Rodi 1987) and if the transport equation is used for temperature the source term represents heat exchange with the surroundings and lateral inflows of cool or hot water.

The width-integrated continuity equation can be depth-integrated analytically to give

$$\frac{\partial A}{\partial t}+\frac{\partial Q}{\partial x}=q_0 \quad \left\{\approx W\frac{\partial \eta}{\partial t}+\frac{\partial Q}{\partial x}\right\} \tag{5}$$

where A (m^2) is the cross-section area and Q ($m^3\,s^{-1}$) is the instantaneous discharge through the cross section. The width-integrated momentum and transport equations cannot be depth-integrated analytically, because we do not have any analytical solutions to the vertical distribution of velocity and density. The velocity distribution in stratified regions can be dominated by the density-driven currents and even be opposite at the bottom and surface. Thus, for example, using a log profile for the velocity distribution is not a satisfactory solution. The model calculates the distributions numerically and thereby we can still depth-integrate the momentum and transport equations numerically.

In the width-integrated momentum equation we assume hydrostatic pressure:

$$p=\int_z^\eta \rho g\mathrm{d}z \tag{6}$$

where ρ ($kg\,m^{-3}$) is the water density and g ($9.81\,m\,s^{-2}$) is the accelaration due to gravity. By use of the Leibniz rule the pressure gradient is determined to be

$$\frac{\partial p}{\partial x}=\rho_S g\frac{\partial \eta}{\partial x}+g\int_z^\eta \frac{\partial \rho}{\partial x}\mathrm{d}z \tag{7}$$

where ρ_S ($kg\,m^{-3}$) is the water density at the surface. The first term on the right-hand side is the barotropic pressure, while the second term is the baroclinic pressure. The internal shear stress is written as

$$\frac{\tau_{zx}}{\rho_0}=\nu_T\frac{\partial u}{\partial z} \tag{8}$$

where ν_T ($m^2\,s^{-1}$) is the turbulent viscosity. A turbulence model can determine this. The bed shear stress is approximated by

$$\frac{\tau_B}{\rho_0}\frac{\mathrm{d}P}{\mathrm{d}z}\approx\left(\frac{d}{D}\frac{g}{C_{xz}^2}|u|u\right)\left(2\sqrt{1+\left(\frac{1}{2}\frac{\mathrm{d}W}{\mathrm{d}z}\right)^2}\right) \tag{9a}$$

where d and D (m) are a local water depth and the maximum water depth, respectively, in a given cross section and u is the velocity in the level z above the considered bed. The Chezy number C_{xz} is related to the normally used Chezy number by boundary layer theory (a log profile, see Eq. (14a)):

$$C_{xz}=C+\frac{\sqrt{g}}{\kappa}\left(1+\ln\left(\frac{z}{D}\right)\right) \tag{9b}$$

where C ($m^{0.5}\,s^{-1}$) is the normally used Chezy number and κ (0.4) is von Kármán's constant.

Sigma coordinate system

The equations are now transformed to a sigma coordinate system. The sigma coordinate is defined by (e.g. Slørdal 1997)

$$\sigma=\frac{z-\eta}{D}=\frac{z-\eta}{\eta-z_B} \tag{10a}$$

where z_B (m) is the bed level. In the pressure term the density influence is, for example, transformed to sigma coordinates as follows:

$$\frac{\partial \rho(x,z,t)}{\partial x} \rightarrow \frac{\partial \rho(x,\sigma,t)}{\partial x} + \frac{\partial \rho(x,\sigma,t)}{\partial \sigma}\frac{\partial \sigma}{\partial x} = \frac{\partial \rho}{\partial x} - \frac{1}{D}\left(\frac{\partial \eta}{\partial x} + \sigma\frac{\partial D}{\partial x}\right)\frac{\partial \rho}{\partial \sigma} \tag{10b}$$

The following width-integrated continuity Eq. (2) is obtained using the above sigma coordinate transformation:

$$\frac{\partial q}{\partial x} - \frac{1}{D}\left(\frac{\partial \eta}{\partial x} + \sigma\frac{\partial D}{\partial x}\right)\frac{\partial q}{\partial \sigma} + \frac{1}{D}\frac{\partial Ww}{\partial \sigma} = \frac{q_0}{\mathrm{d}z} \tag{11a}$$

where $q = Wu$. The momentum Eq. (3) is transformed and rearranged to give

$$\begin{aligned}
&\frac{\partial q}{\partial t} - \frac{1}{D}(1+\sigma)w_S\frac{\partial q}{\partial \sigma} + gW\frac{\rho_S}{\rho_0}\frac{\partial \eta}{\partial x} \\
&- \frac{1}{D^2}\frac{\partial}{\partial \sigma}\left(\nu_T W\frac{\partial q/W}{\partial \sigma}\right) + \frac{d}{D}\frac{g}{C_{xz}^2}\frac{|q|q}{W^2}2\sqrt{1+\left(\frac{1}{2D}\frac{\partial W}{\partial \sigma}\right)^2} \\
&= -\frac{\partial q^2/W}{\partial x} + \frac{1}{D}\left(\frac{\partial \eta}{\partial x} + \sigma\frac{\partial D}{\partial x}\right)\frac{\partial q^2/W}{\partial \sigma} - \frac{1}{D}\frac{\partial qw}{\partial \sigma} \\
&- gW\int_0^\sigma\left(D\frac{\partial \rho/\rho_0}{\partial x} - \left(\frac{\partial \eta}{\partial x} + \sigma\frac{\partial D}{\partial x}\right)\frac{\partial \rho/\rho_0}{\partial \sigma}\right)\mathrm{d}\sigma
\end{aligned} \tag{11b}$$

where w_S is the surface velocity.

Numerical method

The width- and depth-integrated continuity Eq. (5) is approximated in discrete form as follows:

$$W_j^n\frac{\eta_j^{n+1} - \eta_j^n}{\Delta t} + \frac{0.5\left(Q_{j+1}^{n+1} + Q_{j+1}^n\right) - 0.5\left(Q_{j-1}^{n+1} + Q_{j-1}^n\right)}{\Delta x_j + \Delta x_{j+1}} = q_{0j} \tag{12a}$$

also written as

$$\begin{aligned}
&-\frac{0.5}{\Delta x_j + \Delta x_{j+1}}Q_{j-1}^{n+1} + \frac{W_j^n}{\Delta t}\eta_j^{n+1} + \frac{0.5}{\Delta x_j + \Delta x_j}Q_{j+1}^{n+1} \\
&= \frac{0.5}{\Delta x_j + \Delta x_{j+1}}Q_{j-1}^n + \frac{W_j^n}{\Delta t}\eta_j^n - \frac{0.5}{\Delta x_j + \Delta x_{j+1}}Q_{j+1}^n + q_{0j}
\end{aligned} \tag{12b}$$

or

$$\alpha_j Q_{j-1}^{n+1} + \beta_j \eta_j^{n+1} + \gamma_j Q_{j+1}^{n+1} = \delta_j \tag{12c}$$

which is the equation solved in the existing river model.

In the width-integrated momentum Eq. (11b) the terms on the left-hand side are resolved implicitly, while the terms on the right-hand side are resolved explicitly. Term by term we get to the left-hand side of Eq. (11b):

– the local acceleration:

$$\begin{aligned}
\frac{\partial q}{\partial t} &= \frac{q_{j,k}^{n+1} - q_{j,k}^n}{\Delta t} \\
&\quad - \frac{1}{D}(1+\sigma)w_S\frac{\partial q}{\partial \sigma} \\
&= -\frac{\theta}{D_j^n}(1+\sigma)w_{j,kxz}^{n+1}\frac{q_{j,k+1}^{n+1} - q_{j,k-1}^{n+1}}{2\Delta\sigma} \quad - \frac{1-\theta}{D_j^n}(1+\sigma)w_{j,kxz}^n\frac{q_{j,k+1}^n - q_{j,k-1}^n}{2\Delta\sigma}
\end{aligned} \tag{13a}$$

where θ is a temporal weighting coefficient between 0 and 1;

– the barotropic pressure term:

$$gW\frac{\rho_S}{\rho_0}\frac{\partial\eta}{\partial x} = gW^n_{j,k}\frac{\rho^n_{Sj}}{\rho_0}\frac{\theta\left(\eta^{n+1}_{j+1}-\eta^{n+1}_{j-1}\right)+(1-\theta)\left(\eta^{n}_{j+1}-\eta^{n}_{j-1}\right)}{(\Delta x_j+\Delta x_{j+1})}; \tag{13b}$$

– the shear stress term:

$$\begin{aligned}
&-\frac{1}{D^2}\frac{\partial}{\partial\sigma}\left(\nu_T W\frac{\partial q/W}{\partial\sigma}\right)\\
&=-\frac{\theta}{D_j^{n^2}\Delta\sigma^2}\left(\nu^n_{j,k+1/2}W^n_{j,k+1/2}\left(\frac{q^{n+1}_{j,k+1}}{W^{n+1}_{j,k+1}}-\frac{q^{n+1}_{j,k}}{W^{n+1}_{j,k}}\right)-\nu^n_{j,k-1/2}W^n_{j,k-1/2}\left(\frac{q^{n+1}_{j,k}}{W^{n+1}_{j,k}}-\frac{q^{n+1}_{j,k-1}}{W^{n+1}_{j,k-1}}\right)\right)\\
&\quad-\frac{1-\theta}{D_j^{n^2}\Delta\sigma^2}\left(\nu^n_{j,k+1/2}W^n_{j,k+1/2}\left(u^n_{j,k+1}-u^n_{j,k}\right)-\nu^n_{j,k-1/2}W^n_{j,k-1/2}\left(u^n_{j,k}-u^n_{j,k-1}\right)\right);
\end{aligned} \tag{13c}$$

– the bed friction term:

$$\begin{aligned}
&\frac{d}{D}\frac{g}{C^2_{xz}}\frac{|q|q}{W^2}2\sqrt{1+\left(\frac{1}{2D}\frac{\partial W}{\partial\sigma}\right)^2}\\
&\quad=\frac{d_j}{D_j}\frac{g}{C^2_{xz}}\frac{\left|u^n_{j,k+1}\right|q^{n+1}_{j,k+1}}{W^n_{j,k+1}}2\sqrt{1+\left(\frac{1}{2D^n_j}\frac{W^n_{j,k+1}-W^n_{j,k-1}}{2\Delta\sigma}\right)^2}.
\end{aligned} \tag{13d}$$

We will not show the derivative approximations to the terms on the right-hand side as they are not of principal interest and simply denote the contribution by RHST.

The terms can be collected to give

$$\alpha''_{j,k}\eta^{n+1}_{j-1}+\psi''_{j,k}q^{n+1}_{j,k-1}+\beta''_{j,k}q^{n+1}_{j,k}+\zeta''_{j,k}q^{n+1}_{j,k+1}+\gamma''_{j,k}\eta^{n+1}_{j+1}=\delta''_{j,k} \tag{13e}$$

where

$$\alpha''_{j,k} = -gW^n_{j,k}\frac{\rho^n_{Sj}}{\rho_0}\frac{\theta}{(\Delta x_j+\Delta x_{j+1})} \tag{13f}$$

$$\gamma''_{j,k} = gW^n_{j,k}\frac{\rho^n_{Sj}}{\rho_0}\frac{\theta}{(\Delta x_j+\Delta x_{j+1})} \tag{13g}$$

$$\psi''_{j,k} = \frac{\theta}{D^n_j}(1+\sigma)\frac{w^{n+1}_{j,kxz}}{2\Delta\sigma}-\frac{\theta}{D_j^{n^2}\Delta\sigma^2}\frac{\nu^n_{j,k-1/2}W^n_{j,k-1/2}}{W^n_{j,k-1}} \tag{13h}$$

$$\beta''_{j,k} = \frac{1}{\Delta t}+\frac{\theta}{D_j^{n^2}\Delta\sigma^2}\frac{\nu^n_{j,k+1/2}W^n_{j,k+1/2}+\nu^n_{j,k-1/2}W^n_{j,k-1/2}}{W^n_{j,k}} \tag{13i}$$

$$\begin{aligned}
\zeta''_{j,k} &= -\frac{\theta}{D^n_j}(1+\sigma)\frac{w^{n+1}_{j,kxz}}{2\Delta\sigma}-\frac{\theta}{D_j^{n^2}\Delta\sigma^2}\frac{\nu^n_{j,k+1/2}W^n_{j,k+1/2}}{W^n_{j,k+1}}\\
&\quad+\frac{d_j}{D_j}\frac{g}{C^2_{xz}}\frac{\left|u^n_{j,k+1}\right|}{W^n_{j,k+1}}2\sqrt{1+\left(\frac{1}{2D^n_j}\frac{W^n_{j,k+1}-W^n_{j,k-1}}{2\Delta\sigma}\right)^2}
\end{aligned} \tag{13j}$$

$$\delta''_{j,k} = \mathrm{RHST} + \frac{W^n_{j,k}u^n_{j,k}}{\Delta t} + \frac{1-\theta}{D^n_j}(1+\sigma)w^n_{j,kxz}\frac{q^n_{j,k+1}-q^n_{j,k-1}}{2\Delta\sigma}$$

$$- gW^n_{j,k}\frac{\rho^n_{Sj}}{\rho_0}\frac{(1-\theta)\left(\eta^n_{j+1}-\eta^n_{j-1}\right)}{(\Delta x_j + \Delta x_{j+1})} \tag{13k}$$

$$+ \frac{1-\theta}{D^{n\,2}_j\Delta\sigma^2}\left(\nu^n_{j,k+1/2}W^n_{j,k+1/2}\left(u^n_{j,k+1}-u^n_{j,k}\right) - \nu^n_{j,k-1/2}W^n_{j,k-1/2}\left(u^n_{j,k}-u^n_{j,k-1}\right)\right)$$

Using matrix calculations Eq. (13e) can be rewritten to give

$$\alpha'_{j,k}\eta^{n+1}_{j-1} + q^{n+1}_{j,k} + \gamma'_{j,k}\eta^{n+1}_{j+1} = \delta'_{j,k} \tag{13l}$$

and integrating the equation over the depth numerically we get

$$\alpha_j\eta^{n+1}_{j-1} + Q^{n+1}_{j,k} + \gamma_j\eta^{n+1}_{j+1} = \delta_j \tag{13m}$$

which is the equation solved in the existing model (it is noted that $\beta_j = 1$).

The strategy on how to solve the equations can now be explained as follows. In the existing model where the coefficients in Eq. (1) are calculated, this is done in the stratified branches by use of Eqs. (12) and (13). After the water levels and discharges have been determined using the existing source code the vertical distribution of the horizontal velocity is determined by Eq. (13l) and the vertical velocities are then determined by an approximation in discrete form of Eq. (11a).

Results

Tests on the implementation in MIKE 11 are outlined in the following to show that the model can simulate different engineering flow problems.

Logarithmic velocity profile

In this test we compare our numerical solution to an analytical solution, i.e. the logarithmic velocity profile. In the momentum equation the important terms are the barotropic pressure, internal shear stress and bed friction terms. It is remarked that in the next test we compare the numerical solution to measurement, testing the same terms plus the surface friction.

The logarithmic velocity profile can be derived analytically assuming a linearly growing mixing length from the bed and a constant shear stress equal to the bed shear stress, i.e. where the largest velocity gradients are located. Thus an identical profile cannot and should not be obtained by numerical models. Still, the profile has proven to be a good approximation to measurements. The logarithmic velocity profile is an important part of the basis of river modelling as it is used to derive the formulation of the bed friction and resistance radius. Thus it is important to make sure that the model solution approximates the logarithmic velocity profile.

The logarithmic velocity profile is determined by

$$\frac{u}{U_f} = \frac{1}{\kappa}\ln\left(\frac{z}{k/30}\right) \tag{14a}$$

where U_f (m s^{-1}) is the friction velocity and k (m) is Nikuradse's roughness. The analytical turbulent viscosity profile is determined by

$$\frac{\nu_T}{\kappa U_f D} = \frac{z}{D}\left(1-\frac{z}{D}\right) \tag{14b}$$

as can also be compared to the numerically obtained viscosity. The numerical test was set up for a wide channel with a slope I = 5 m/5000 m, a constant water depth D = 2 m and

a Chezy number $C = 36\,\mathrm{m}^{1/2}\,\mathrm{s}^{-1}$. The combined water depth and Chezy number corresponds to $k = 0.25$ m. The $k-\varepsilon$ turbulence model was chosen for the model test. The friction velocity $U_f = (gDI)^{1/2}$ by which the expected profiles can be determined using Eqs. (14a, b), see Figure 1. As mentioned above the logarithmic velocity profile is known to be only an approximation to the correct velocity profile. The biggest uncertainty in the analytical viscosity profile is in the middle of the water column, because of the assumptions applied when deriving the profile, or exactly where we find disagreement between the solutions. For that reason the comparisons in Figure 1 are considered to show a reasonable agreement.

Wind driven velocity profile

In this test we compare our numerical solution to experimental data. In the momentum equation the important terms are the barotropic pressure, internal shear stress and surface friction terms.

Several numerical tests were made with different length–depth scales, and provided equal dimensionless results. Thus the dimensions of the actual setup are not important. The numerical test presented was set up for a 500 m long wide channel. The water depth $D = 2$ m and a Chezy number $C = 36\,\mathrm{m}^{1/2}\,\mathrm{s}^{-1}$. The combined water depth and Chezy number corresponds to $k = 0.25$ m. The wind speed was $2.5\,\mathrm{m\,s}^{-1}$. The $k-\varepsilon$ turbulence model was chosen for the model test. The comparisons to measurements show a good agreement, see Figure 2.

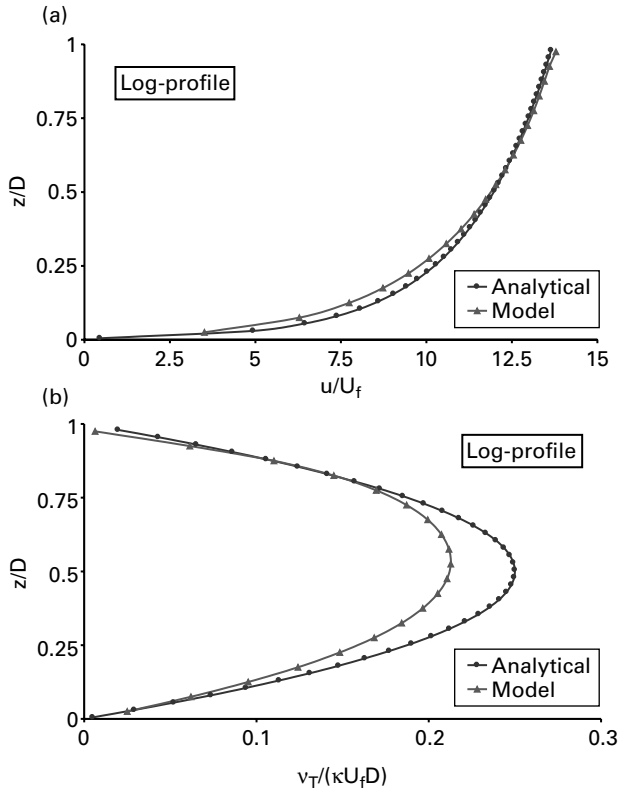

Figure 1 (a) Comparison of logarithmic and calculated vertical velocity profile. (b) Comparison of the expected and calculated viscosity profiles

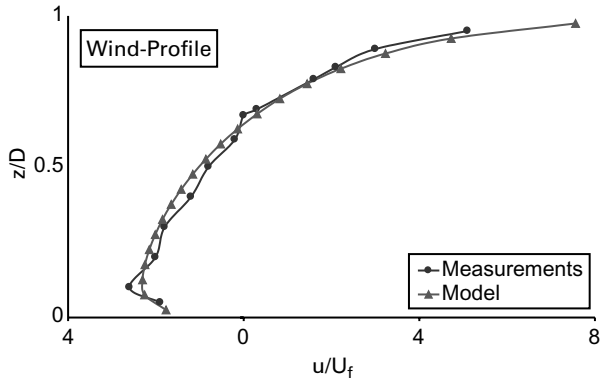

Figure 2 Comparison of measured (Baines and Knapp 1965) and calculated wind driven vertical velocity profile

Rapid accelerated flow in channel

In this test we will compare two numerical solutions, i.e. simulated rapid accelerated flow by MIKE 11 with and without vertical resolution. In the momentum equation the important terms are the acceleration, barotropic pressure, internal shear stress and bed friction terms.

MIKE 11 without vertical resolution is known to produce good results for this case. From the test on the logarithmic velocity profile we know that the solutions with and without vertical resolution will not be identical. We are not interested in knowing whether or not MIKE 11 with vertical resolution produces better results, as the purpose of the vertical resolution is to produce better results in stratified water bodies, but we want the solutions to be close as MIKE 11 produces reasonably results. This is especially important if a water body is only stratified part of the time and at connections between branches with and without vertical resolution.

The test was set up as outlined under logarithmic velocity profile. The boundary conditions in each end are specified as water level boundaries, whereby the discharge is calculated by the model. Initially the water surface is horizontal. The water surface is rapidly lowered at the downstream boundary. The results are shown in Figure 3. The comparison of the discharges show good agreement. When constant discharge is reached the solution with vertical resolution shows slightly higher discharge than in the case without vertical resolution.

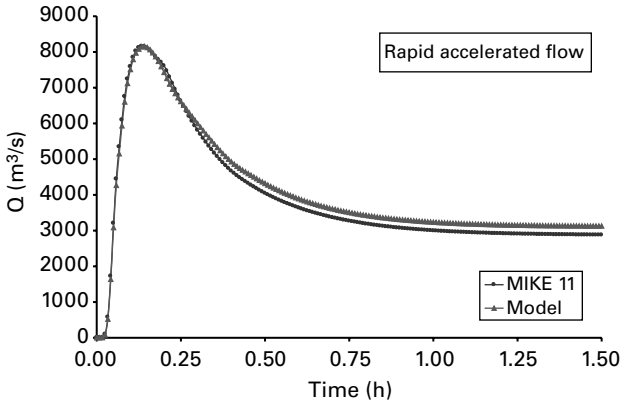

Figure 3 Comparison of discharge obtained by MIKE 11 with and without vertical resolution for a rapidly accelerated flow in a channel

Lock exchange

In this test we compare our numerical solution to an analytical solution, i.e. the lock-exchange speed. In the momentum equation the important terms are the local acceleration term and the barotropic and baroclinic pressure terms.

The analytical solution is based on potential theory and predicts a speed of the head of (e.g. Pedersen 1986)

$$U_t = 0.5\sqrt{\Delta g D} \tag{15}$$

where U_t ($\mathrm{m\,s^{-1}}$) is the speed of the head and Δ is the dimensionless reduced density. This solution has been successfully compared to measured speeds: actually it provides an upper bound on the head speeds, and is considered to be satisfactory for our purpose.

The numerical test was set up for a 500 m long wide channel with a water depth $D = 10$ m, a Chezy number $C = 45\,\mathrm{m^{1/2}\,s^{-1}}$ and a constant turbulent viscosity of 0. The initial temperature was specified to be 5, 10, 15, 20, 25 or 28°C on the first 250 m and always 30°C on the last 250 m. We expect the numerical solution to give slightly lower head speeds than the analytical solution for two reasons. Firstly because the analytical solution is known to provide a good solution, but on the high side, i.e. to be an upper bound. Secondly because the flow features involves two moving vertical fronts as we do not and cannot resolve satisfactorily. Tests were made, but are not shown, to see the effect of improving the horizontal resolution in the model setup. The tests showed that improving the horizontal resolution leads to better agreement between the analytical solution and the model results (but of course in practical situations our horizontal resolution is limited by computational time). It is noticed that the shapes of the two line matches, see Figure 4. For these reasons the comparison are considered to show a reasonable agreement.

Wind-forced entrainment

In this test we compare our numerical solution to an analytical–empirical solution. In the momentum equation the important terms are the barotropic and baroclinic pressure terms and the shear stress term.

The numerical test was set up for a 5000 m long wide channel with an initial water depth $D = 30$ m and a Chezy number $C = 45\,\mathrm{m^{1/2}\,s^{-1}}$. The wind speed was $7\,\mathrm{m\,s^{-1}}$. The initial temperature was linearly distributed over depth with 5°C at the bed and 25°C at the surface. The k–ε turbulence model was chosen for the model test with no Richardson damping (Rodi 1987).

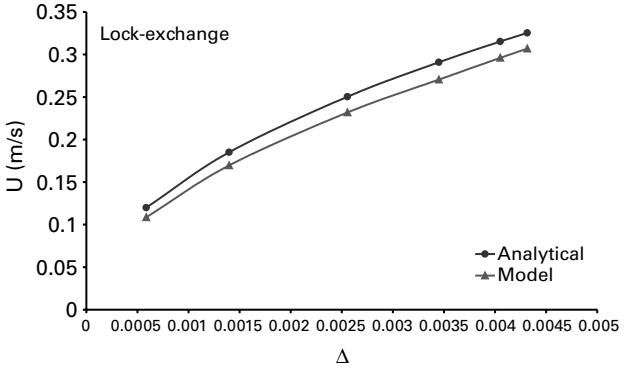

Figure 4 Comparison of analytical solution (actually upper bound on speed) and model results from the lock-exchange numerical experiment. The horizontal resolution in the model is 2.5 m

On the basis of bulk flux Richardson number theory (Pedersen 1986; Møller *et al.* 1997) an analytical–empirical solution to the interface position can be found (Jakobsen and Larsen 1989):

$$t = Ah^3 + Bh \tag{16}$$

and

$$A = -\frac{0.5a_T(T_S - T_B)g}{153.3R_f^T DU_f^3}$$

$$B = \frac{6}{51.1R_f^T U_f}$$

where h (m) is the interface position, a_T ($-1.35 \times 10^{-4}\,\mathrm{K}^{-1}$) is the expansion coefficient, T (K) is the temperature, the index S and B are for surface and bed, respectively, and R_f^T is the bulk flux Richardson number (from 0–4.5%).

The comparison between the analytical–empirical solution with $R_f^T = 1.5\%$ and the modelling show good agreement, see Figure 5. By changing the value of the constant $c_{3\varepsilon}$ in the k–ε turbulence model it is possible to change the development of the thermocline, i.e. fit different values of the bulk flux Richardson number R_f^T. It should be remembered that the analytical-empirical solution is rather crude, not taking, for example, the horizontal velocity distribution into account. As the upper layers deepens we expect the entrainment in the numerical model to slow down as the growth of the boundary layer becomes more and more important.

Discussion

One can always do more to verify the implementation of a numerical scheme. In the tests presented we have investigated the acceleration term, the barotropic and baroclinic pressure terms, the internal shear stress and the surface and bed frictions terms. The numerical solutions showed good agreement with analytical solutions, experiments or other numerical solutions. The analytical solutions can always be questioned, but they were all well-known solutions and considered precise enough solutions for our purpose. We did not focus our test in this paper on natural rivers. The only difference between the tests presented here and tests on natural rivers systems is the arbitrarily shaped cross sections. The procedures to handle the geometry in MIKE 11 is well established and used in the implementation. Still this kind of test takes place in practical engineering projects. Thus we consider the verification successful.

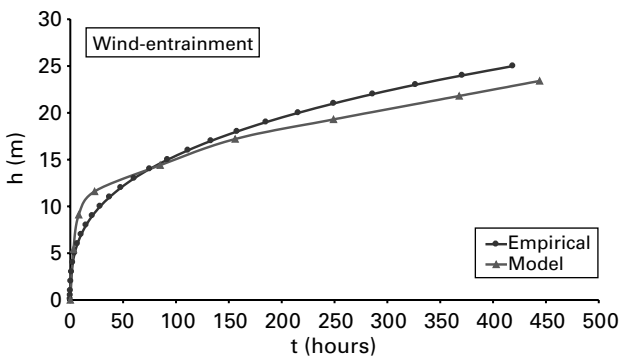

Figure 5 Comparison of analytical–empirical solution and model results from the wind-forced entrainment numerical experiment

Conclusion

A simple method to extend an existing river model to include vertical resolution is outlined and implemented in MIKE 11. The method is shown to work by testing the implementation on several simple test cases: logarithmic velocity profile, wind driven velocity profile, rapidly accelerated flow, lock exchange and wind-forced entrainment. All test cases gave good agreement. Inclusion of vertical resolution in a river model can improve the model solution in areas where the velocity profile is non-logarithmic. The velocity distribution can, for example, be non-logarithmic in regions where the water column is stratified, as is often the case in reservoirs, estuaries and lakes, for example.

References

Abbott, M.B. (1979). Computational hydraulics, elements of the theory of free surface flows. *Monographs and Surveys in Water Resources Engineering* (vol 1), Pitman, London.

Abbott, M.B. and Ionescu, F. (1967). On the numerical computation of nearly-horizontal flows. *J. Hydr. Res.*, **5**(2), 97–117.

Baines, W.D. and Knapp, D.J. (1965). Wind driven water currents. *J. Hydr. Div.*, **91**(HY2), 205–221.

Cunge, J.A., Holly, F.M. and Verwey, A. (1980). Practical aspects of computational river hydraulics. *Monographs and Surveys in Water Resources Engineering* (vol 3), Pitman, London.

Jakobsen, Fl. and Larsen, T.E. (1989). One dimensional $k-\varepsilon$ modelling of a surface layer. Progress Report 69. Inst. Hydrodyn. and Hydraulic Eng., Technical University, Denmark, pp 9–20.

Møller, J.S., Ottesen Hansen, N.-E. and Jakobsen, Fl. (1997). Mixing in stratified flow caused by obstacles. *J. Marine Environ. Engng*, **4**, 97–111.

Pedersen, Fl.B. (1986). Environmental hydraulics: stratified flows. *Lecture Notes on Coastal and Estuarine Studies* (**vol 18**), Springer-Verlag, Berlin.

Rodi, W. (1987). Examples of calculation methods for flow and mixing in stratified fluids. *J. Geophys. Res.*, **92**(C5), 5305–5328.

Slørdal, L.H. (1997). The pressure gradient force in sigma-co-ordinate ocean models. *Int. J. Numer. Meth. Fluids*, **24**, 987–1017.